

# Accelerated T2 Prime Mapping using Dynamic Compressed Sensing with Patch-based Low-Rank Penalty

Dongwook Lee<sup>1</sup>, Eung Yeop Kim<sup>2</sup>, Huisu Yoon<sup>1</sup>, Sunghong Park<sup>1</sup>, and Jong Chul Ye<sup>1</sup>

<sup>1</sup>Korea Advanced Institute of Science and Technology, Daejeon, Korea, <sup>2</sup>Gachon University Gil Medical Center, Incheon, Korea

## Purpose

T2 prime (T2') mapping is an application of parametric magnetic resonance imaging (MRI) technique for diagnosis of brain diseases such as ischemic stroke and occlusive carotid disease. Recently, T2' imaging was proposed as a better way to predict infarct growth in acute stroke than Diffusion Weighted Imaging (DWI) which was commonly used.<sup>[1]</sup> Because T2' map is T2\* mapping with correction for T2 relaxation effects, it may provide useful information of blood oxygenation that is not affected by signal changes caused by gliosis or edema. However, the quantitative measure of parameter maps with high resolution requires the acquisition of multiple images using different sequence parameters such as echo time (TE). That is usually associated with long acquisition times although time saving is the most important thing in acquisition of MRI in acute ischemic stroke because therapy should be given to patients as soon as possible. Therefore, to reduce the acquisition time of MR data, we use a compressed sensing algorithm using patch based low rank penalty.<sup>[2]</sup> for the reconstruction of T2 and T2\* weighted images to obtain the T2 prime map.

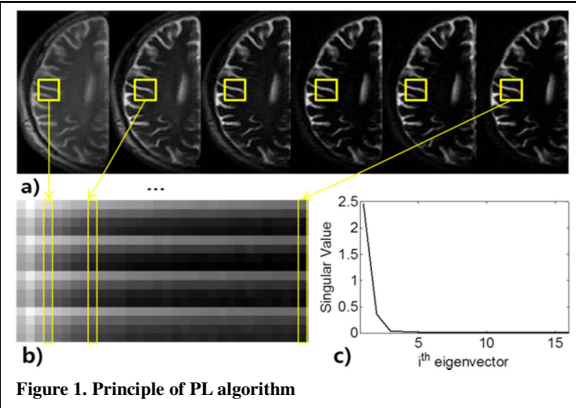


Figure 1. Principle of PL algorithm

## Methods

The sets of T2 weighted (T2W) images and T2\* (T2\*W) weighted images of human brain were acquired at multiple TEs in Cartesian coordinate with 3T MR scanner (Siemens; Verio). The following parameters were used for the T2 measurement: SE sequence with 32 echoes, 20 ms echo spacing (ESP), TR 4 sec, FOV 172x230 mm, 5-mm slice thickness, 128x96 matrix, 6 slices and 4 coils. The T2\* mapping parameters are as follows: GRE sequence with 12 echoes, 2 ms ESP, and the remaining parameters are same with those of T2 acquisition parameters. To verify the performance of the algorithm, reconstructions of downsampled data are compared to images from full data. For the proposed method, k-t FOCUSS is first used for an initial reconstruction.<sup>[3]</sup> After that, patch based low rank (PL) algorithm is applied to improve the reconstruction quality by exploiting the self-similarities along temporal directions.<sup>[2]</sup> More specifically, as shown in Fig.1, the group of patches along temporal directions has low rank structures due to their geometric similarity. Our patch-based low rank algorithm minimizes the following augmented cost function:  $C(W, x) = ||y - Fx||^2 + \sum_p \lambda_p \left\{ \frac{1}{\mu} ||V_p(x) - W_p||_F^2 + ||W_p||_{g_{\mu, \nu}} \right\}$  where  $y$  is a k-t space data,  $F$  is a 2-D Fourier sampling operator, and  $x$  represent unknown spatio-temporal images. The second term corresponds to the augmented function with augmented variable  $W_p$ , which is derived using half-quadratic regularization technique for Huber-based non-convex low

rank penalty for the temporal patch groups  $V_p$ . The similarity patch groups are obtained using overlapping patches. The solutions  $x^{(k)}$  and  $\{W^{(k)}\}$  are resolved by alternating minimization. Due to the non-convexity, the final solution depends on the initialization. Resultingly, four different algorithms are compared for T2' mapping: k-t FOCUSS, k-t FOCUSS with KLT, PL algorithm after k-t FOCUSS and PL algorithm after k-t FOCUSS with Karhunen-Loeve transform (KLT). Then, a pixel-wise fitting of the signal intensities to an exponential decay function is used to obtain the relaxation times, T2 and T2\*. To investigate the effects of the downsampling, fully sampled datasets were undersampled retrospectively with reduction factors of 2, 4, 6, 8 for the T2 and 2 for T2\* dataset. The mean square error (MSE) was calculated to measure the quality of reconstructions.

## Results

k-t FOCUSS with KLT (Fig.2 c, g) reconstructs better images than the images from k-t FOCUSS (Fig. 2. b, f) because the T2\* data is represented more sparsely on KLT domain. The results of patch based low rank algorithm are represented on Fig. 2 d-e, h-i, which showed better reconstruction than k-t FOCUSS with KLT alone. In Fig. 3, the reconstruction of T2', T2\* and T2 map from downsampled data are displayed. For calculating T2' map, we found that different acceleration scheme for T2 and T2\* are appropriate without affecting the accuracy of final T2' maps. This is because that T2\* images have much faster decays with spatial variations perhaps due to susceptibility artifacts, which are difficult to sparsify compared to T2 maps. Therefore, we found that the acceleration rate x8 for T2 is still good enough whereas the rate x2 for T2\* provided valuable result. By combining two different acceleration schemes, the overall T2' map acquisition can be significantly reduced.

## Conclusions

In this study, we have presented a CS-MRI reconstruction method for T2' mapping from highly undersampled dynamic MR data. Prior knowledge of the signal was incorporated in reconstruction by using k-t FOCUSS KLT and patch based low rank algorithm. The proposed algorithm produced accurate result at high reduction factors in T2, T2\* and T2' mapping. In the given limited scan time, this acceleration may increase the spatial or temporal resolution in dynamic MRI. Further studies are needed to accelerate T2\* image acquisition without susceptibility artifact using z-shimming correction.

## References

[1] Siemonsen, S et al., T2 imaging predicts infarct growth beyond the acute diffusion weighted imaging lesion in acute stroke. *Radiology*, 2008; 248(3): 979-986. [2] Yoon, H et al., Motion compensated compressed sensing dynamic MRI with low rank patch-based residual reconstruction. *ISBI*, 2013; 314-317 [3] Jung, H et al., k-t FOCUSS: A general compressed sensing framework for high resolution dynamic MRI. *Magnetic Resonance in Medicine*, 2009; 61(1): 103-116

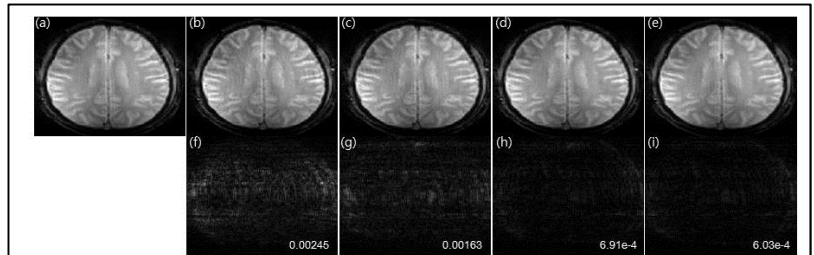


Figure 2. Comparison of reconstruction for T2\* images (6<sup>th</sup> z-slice, 6<sup>th</sup> Echo, b-e), MSE and difference images (f-i) from original full data (a)

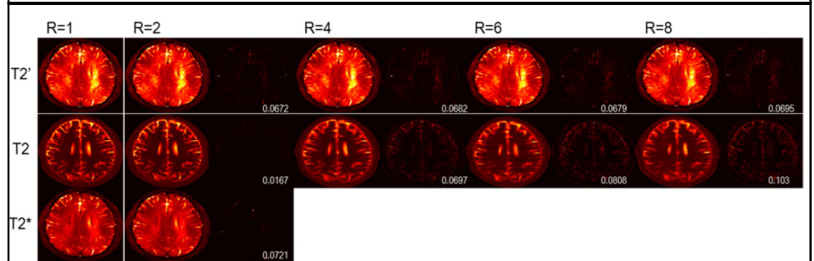


Figure 3. Reconstruction maps of T2', T2 and T2\*. Difference maps from full data and MSE are displayed next to each reconstruction maps.